The Journal of the Korean Society of Oceanography
Vol. 32, No. 1, pp. 8-16, March 1997

Application of the Ventilation Theory to the East Sea

YOUNG HO SEUNG
Department of Oceanography, Inha University

The ventilation theory developed by Luyten, Pedlosky and Stommel (1983) is applied to the East Sea to understand the general circulation pattern of the Intermediate Water, especially the ventilated circulation beneath the Tsushima Warm Current. The original model is slightly modified such that it takes the inflow-outflow of the Tsushima Current into consideration. Results of the model indicate that for sufficiently strong Ekman pumping, the Intermediate Water circulates cyclonically by ventilation. The Intermediate Water subducts beneath the Tsushima Warm Water through the western boundary layer. Off the western boundary layer, it turns northward, outcrops to the north by passing the polar front and continues to flow northward until it finally is absorbed by the northern boundary layer. This result seems to be compatible with some recent observations. Over the ventilated area, the transport of the Tsushima Current is negligible and most transport occurs in the shadow area where the Intermediate layer is motionless indicating that, over the deep motionless layer, the two-layered vertical structure under consideration becomes substantially single-layered.

INTRODUCTION

The East Sea is a marginal sea in the Northwest Pacific. From the geographical point of view, the northern part of the basin belongs to the subpolar region and the southern part to the subtropical region with the former slightly larger than the latter. Through the southern inlet, a warm current originating from the Kuroshio, called the Tsushima Current (briefly TC), enters the basin and flows out through the northern outlets into the subpolar region. A part of the warm current, called the East Korean Warm Current, flows northward along the Korean coast. It separates from the coast and flows in nearly zonal direction toward the outlets. Further south, a part of the TC flowing along the Japanese coast, called the Nearshore Branch, is known to be topographically trapped (Yoon, 1982b). In the north, a cold current, called the Liman Current or the North Korean Cold Current, flows southward along the Siberian/Korean coast. The boundary between the warm and cold waters form a polar front (Fig. 1). The surface of the basin is known to be affected largely by positive wind stress curl, which is maximum near the northern boundary (Na *et al.*, 1992).

Below the TC water, the Intermediate Water (briefly IW) characterized by minimum salinity and maximum dissolved oxygen is found, which seems to be connected to the surface north of the polar front (Fig. 2). The IW here comprises the classical one (Moriyasu, 1972) and the one found by Kim and Chung (1984) off Korean coast. The latter one, named the East Sea Intermediate Water (briefly ESIW), is richer in dissolved oxygen than the former but these two water masses might be classified as the same one (Fig. 3). The ESIW may be formed more recently than the other. Beneath the IW, a deep homogeneous water called the Japan Sea Proper Water (briefly DW) is found. Further details of general hydrography can be found in Moriyasu (1972).

According to Senjyu and Sudo (1994), the upper portion of the DW just below the IW nearly outcrops to the northwest of the basin, suggesting that this is the source region of the water mass considered. They also show that this water mass circulates cyclonically around the basin. In fact, an indication of deep convection is reported by Seung and Yoon (1995a). The cyclonic circulation of the deep water is also compatible with the observation in Kim and Chung (1984) because the ESIW, which is richer in oxygen than that found eastward, occupies the upstream portion of this circulation. Cho and Kim (1994) suggest, however, that the ESIW found off the Korean coast comes through two distinct paths: one from the north along the

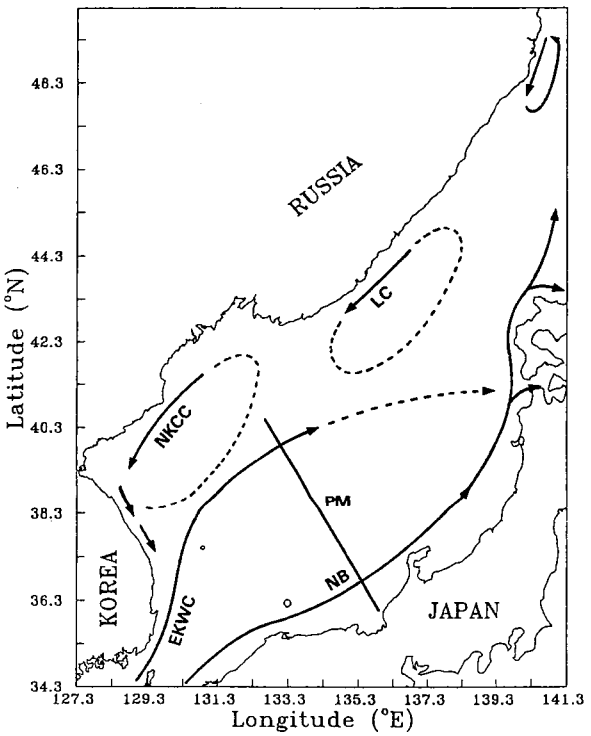

Fig. 1. A schematic diagram of the East Sea circulation (after, Uda, 1934). LC means Liman Current; NKCC, North Korean Cold Current; EKWC, East Korean Warm Current; NB, Nearshore Branch. PM is the observation line occupied by Maizuru Marine Observatory (MMO).

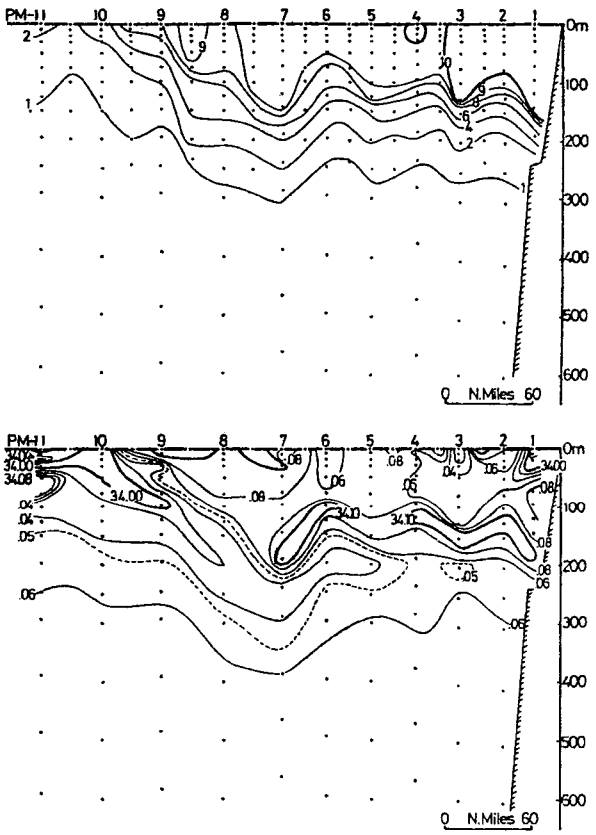

Fig. 2. Vertical sections of temperature (in°C) and salinity (in psu) obtained in March, 1976 along the line PM. Station 9 (39° 47'N, 133° 12'E) is the approximate position of the polar front. See Fig. 1 for location. After MMO (1976).

western boundary of the basin and the other from the northeast.

Circulation of the East Sea has long been studied both numerically and analytically (Yoon, 1982a and 1982b; Kang, 1988; Seung, 1992; Seung and Kim, 1993, Seung and Yoon, 1995b). The models used in the previous studies give relatively satisfactory results for the surface circulation. However, the dynamics of the intermediate and deep circulations are still unclear. It is therefore necessary to outline the possible circulation pattern of the intermediate/deep water as a first step before more serious attempts are to be made. For this purpose, a simple analytic model similar to the initial ventilation theory (Luyten *et al.*, 1983; briefly LPS) is applied to the East Sea.

MODEL FORMULATION

Idealize the East Sea as a rectangular basin which consists of three layers: the TC water, the IW and the DW from the surface. The TC water enters the interior of the basin from the western boundary layer and flows out through the outlet on the eastern boundary (Fig. 4). The outlet is very narrow extending from y_2-δ to y_2 where y_2 is the outcrop latitude of the IW as mentioned later and δ is the width of the outlet assumed to be very narrow. For simplicity, only the ocean interior is considered excluding the western and northern boundary layers. Take x and y coordinates directing eastward and northward, respectively. Since only the circulation of the IW is interested, the DW layer is assumed infinitely deep and therefore motionless. The origin is taken at the point where the southern boundary and the outer limit of the western boundary layer meet. The bottom depth of the IW is H_0 when it is undisturbed by local forcing. The interface between the TC and IW layers, however, is assumed to outcrop along the latitude y_2. This assumption is similar to one taken by LPS. The two assumptions are different, however, because the one by LPS is induced by the surface heat flux whereas the present one is induced by the inflow-outflow of the TC as seen below. In this model, the surface heat flux is therefore not con-

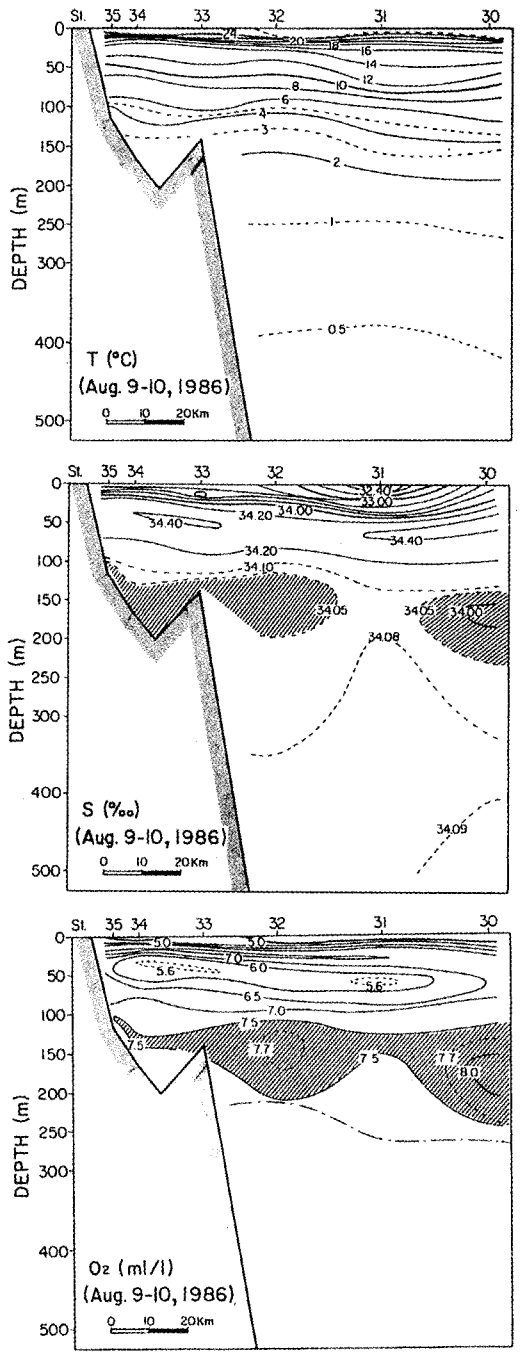

Fig. 3. Vertical sections of (a) temperature, (b) salinity and (c) oxygen along 36° 30'N in August 9~10, 1986. Shaded areas denote salinity minimum and oxygen maximum. After Kim *et al.* (1991).

sidered by taking only the wind stress curl into account.

The governing equations are those for geostrophic relationship

$$v_1 = \frac{1}{f_0}\frac{\partial}{\partial x}[g'_{12}h_1 + g'_{23}(h_1+h_2)] \tag{1}$$

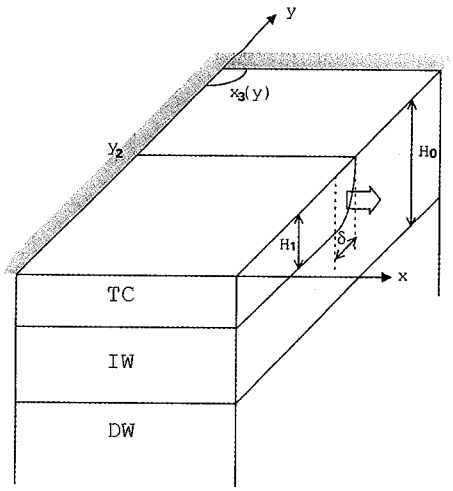

Fig. 4. Idealized model domain. The Tsushima Current (TC) flows out through the outlet located between y_2-δ and y_2 on the eastern boundary. South of y_2-δ along the eastern and southern boundaries, thickness of the TC layer is constant at H_1. North of y_2 along the eastern boundary, it vanishes. The bottom depth of the IW (Intermediate Water) is H_0 along the eastern and southern boundaries. The Deep Water (DW) has infinite depth and outcrops west of $x_3(y)$. The line y_2 is the outcrop latitude of the IW.

$$v_2 = \frac{g'_{23}}{f_0}\frac{\partial}{\partial x}(h_1+h_2) \tag{2}$$

and for Sverdrup balance

$$\beta(v_1 h_1 + v_2 h_2) = f_0 w_E \tag{3}$$

where v is the y-component of velocity, g' the reduced gravity between the two layers considered, f_0 the representative value of the Coriolis parameter, h the layer thickness, β the beta constant, w_E the Ekman pumping velocity with subscript numbers denoting the layers ordered from the surface.

Since there is no normal flow across the eastern and southern boundaries, the layer thickness should be constant along these boundaries. Due to the outflow, however, a discontinuity in layer thickness of TC is expected across the outlet. Thus we take the boundary conditions as follows:

$$h_1(x,0)+h_2(x,0) = h_1(x_E,y)+h_2(x_E,y) = H_0 \tag{4}$$

$$\begin{aligned} &h_1(x,0) = h_1(x_E,y) = H_1 && \text{for } y < y_2-\delta \\ &h_1(x_E,y) = H_1(y_2-y)/\delta && \text{for } y_2-\delta \le y \le y_2 \\ &h_1(x_E,y) = 0 && \text{for } y > y_2 \end{aligned} \tag{5}$$

where subscript E denotes the eastern boundary.

For convenience, the layer thickness of TC is

assumed to vary linearly within the narrow outlet. The condition for the TC taken here is different from that of LPS because of the inflow-outflow condition considered here.

First consider the case where there is no wind forcing. Without local forcing, the IW cannot be activated except the TC induced by the inflow-outflow. From (3), no meridional current is possible for both the IW and TC water. Integrating (2) with respect to x from x to x_E with the boundary condition (4), gives the uniform bottom depth of the IW, i.e., $h_1+h_2=H_0$. Integrating (1) with the condition (5), results in the zonally uniform depth of the TC water, i.e., it has the same meridional distribution as shown by (5). Thus the TC pattern, as well as the polar front, depends exclusively on the outflow boundary condition. Outcropping of the IW, or the polar front, occurs along the latitude y_2. For simplicity, it is assumed that this outcropping line does not change by the local wind forcing. In LPS, the outcropping of the subsurface water is also assumed parallel to the latitude line, where it is implicitly assumed to be maintained by surface heat flux.

For w_E not vanishing, the solutions of (2) and (3) for $y>y_2$ are

$$h_1 = 0 \tag{6}$$

$$h_2^2 = H_0^2 - D_0^2\,(x,y) \tag{7}$$

where

$$D_0^2\,(x,y) = \frac{2f_0^2}{\beta g'_{23}} \int_x^{x_E} w_E\,(x,y)\,dx \tag{8}$$

which simply becomes

$$D_0^2\,(x,y) = \frac{2f_0^2 w_E\,(y)}{\beta g'_{23}}\,(x_E - x) \tag{9}$$

when w_E is independent of x. For positive w_E, D_0 is positive and the layer thickness decreases westward from H_0 at the eastern boundary and vice versa. For sufficiently large w_E, therefore, outcropping of the DW occurs west of the point where D_0 becomes the same as H_0. For w_E decreasing southward, outcropping of the DW occurs west of $x_3(y)$ as shown in Fig. 4. For negative curl, however, the layer thickness increases westward from H_0.

In the region $y<y_2$, the IW layer is shielded from the direct wind forcing. Substituting (1) and (2) into (3) leads to

$$\frac{g'_{12}}{g'_{23}} h_1^2 + (h_1+h_2)^2 = \frac{g'_{12}}{g'_{23}} h_1^2\,(x_E,y) + H_0^2 - D_0^2 \tag{10}$$

Relationship between h_1 and h_2 can be obtained in the same way as that by LPS. Since the potential vorticity is conserved, both its isolines and isobars coincide with the trajectories of water particles, i.e.,

$$\frac{f}{h_2} = G\,(h_1+h_2) \tag{11}$$

where $G(h_1+h_2)$ is an arbitrary function of h_1+h_2, which is proportional to the pressure of the IW layer. For those trajectories crossing the outcropping latitude y_2, the potential vorticity at that latitude is $f_2/(h_1+h_2)$, where f_2 is f at y_2. For these trajectories, therefore, it follows that

$$G\,(h_1+h_2) = \frac{f_2}{h_1+h_2} = \frac{f}{h_2} \tag{12}$$

which gives

$$h_1 = (1-\frac{f}{f_2})(h_1+h_2) \tag{13}$$

Introducing (13) to (10) leads to

$$(h_1+h_2)^2 = \left[\frac{g'_{12}}{g'_{23}} h_1^2\,(x_E,y) + H_0^2 - D_0^2\right] \Big/ \left[\frac{g'_{12}}{g'_{23}}(1-\frac{f}{f_2})^2 + 1\right] \tag{14}$$

In the shielded area, the IW cannot move along the eastern boundary while conserving the potential vorticity because it should have the same thickness H_0 along this boundary. Therefore, an area sheltered from the ventilation is expected to occur near the eastern boundary; this area is named shadow area. The easternmost trajectory separating the ventilated area from the shadow area should pass through the eastern end of the outcropping line, i.e., the point (x_E, y_2), where $h_1+h_2=H_0$. This trajectory can be found by letting $h_1+h_2=H_0$ in (14). The result is

$$(1-\frac{f}{f_2})^2 H_0^2 = \left[h_1^2(x_E,y) - \frac{g'_{23}}{g'_{12}} D_0^2\{x_2(y),y\}\right] \tag{15}$$

where $x_2(y)$ denotes the trajectory to be found. East of $x_2(y)$, only the TC layer is in motion. In this area, applying (1) to (3) with $h_1+h_2=H_0$ and $v_2=0$ leads to

$$h_1^2 = h_1^2(x_E, y) - \frac{g'_{23}}{g'_{12}} D_0^2 \tag{16}$$

Continuity of h_1 along $x_2(y)$ is assured because the two values of h_1 obtained by using (13) and (16) along $x_2(y)$ are found to be the same.

APPLICATION TO THE EAST SEA

Under the positive wind stress curl which prevails in the East Sea, the IW exposed directly to the wind forcing will make a cyclonic circulation consisting of the northward interior flow indicated by (7) and the reversed western boundary current implicitly assumed in this model. For wind forcing extending to the south of the outcropping latitude, y_2, a ventilated northward movement of the submerged IW is expected from (14). The trajectories emanate from the western boundary layer, obduct across the outcrop latitude y_2, and are absorbed into the northern boundary layer. For reference, it should be mentioned that for negative wind stress curl, the ventilation of the IW beneath the TC water is impossible in this basin. For that to be possible, there should exist a trajectory $x_2(y)$ satisfying (15) in the region $y<y_2-\delta$. In this relatively small basin, however, $(1-f/f_2)$ of (15) is on the order of 10^{-5} while $h_1(x_E, y)$ is on the same order as H_0. Therefore, the right hand side of (15) should practically vanish. This is impossible because D_0^2 is negative in this case.

Table 1. Typical parameter values of the East Sea

parameter	value
x_E	1×10^6 m
y_N	1.2×10^6 m
y_2	0.8×10^6 m
δ	10^4 m
H_1	10^2 m
H_0	4×10^2 m
w_0	$\leq10^{-6}$ m/sec
f_0	10^{-4} sec^{-1}
g'_{23}	2×10^{-2} m/sec^2
g'_{12}	1.7×10^{-1} m/sec^2
β	10^{-11} m^{-1}sec^{-1}

For more quantitative description, the Ekman pumping, or equivalently the wind stress curl, should be defined in more specific form. The zonally-averaged wind stress curl is largely positive in the East Sea and decreases nearly linearly southward with maximum Ekman pumping w_0 about 5×10^{-6} m/s appearing in February and nearly vanishing in summer (Na *et al.*, 1992). For simplicity, w_E is approximated as a linear function of y:

$$w_E = w_0(y-y_e)/(y_N-y_e) \tag{17}$$

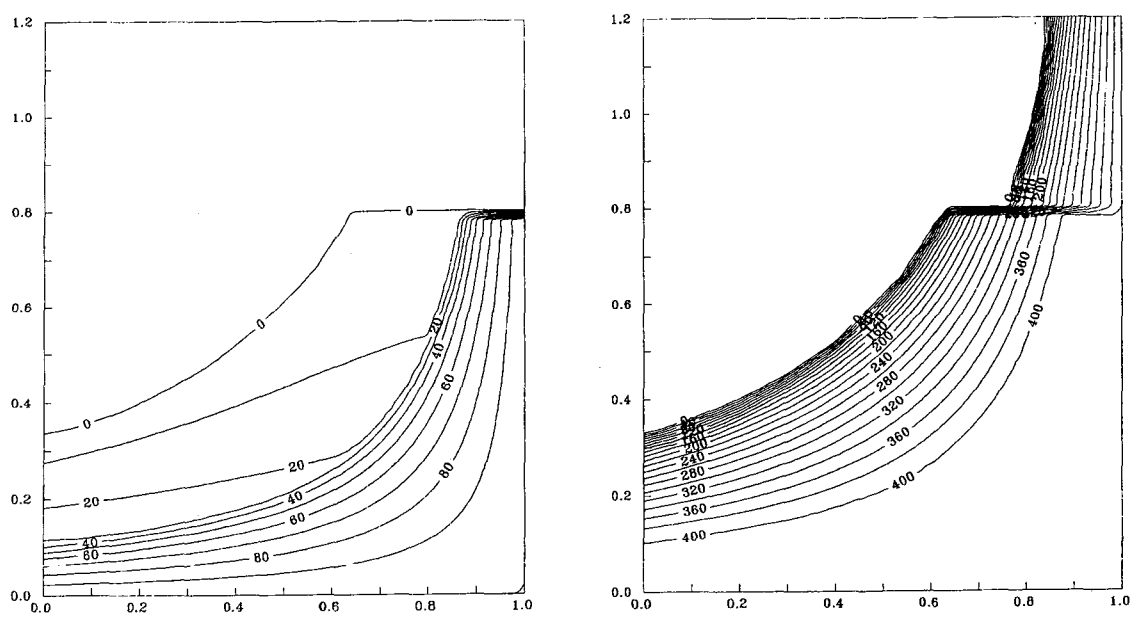

Fig. 5. Distributions of the bottom depths (in meter) of the TC (left) and IW (right) layers for $w_0=10^{-6}$ m/s and $y_e=0$. Eastward and northward axis are normalized by the east-west dimension of the basin, x_E. The outcrop latitude y_2 is taken as 0.8.

where w_0 is the maximum Ekman pumping velocity found in the north of the basin, y_N the meridional dimension of the basin and y_e the latitude where w_E vanishes. For comparison, Ekman pumpings having different distribution and magnitude, i.e., different w_0 and y_e, are considered. Other parameters which can be considered as typical of the basin are shown in Table 1.

For $w_0=10^{-6}$ m/s and $y_e=0$, the wind effect appears so strong that the DW outcrops in large area northwest of the basin (Fig. 5). The transport patterns are similar to the distributions of the bottom depth of the TC and IW, respectively (Fig. 6). Large amount of IW emanates from the western boundary layer below the TC water, outcrops at latitude y_2, continues to flow northward, and finally joins the northern boundary layer. The transport of the IW is larger than that of TC. It is implicitly assumed that the IW makes a closed circulation by flowing along the northern and western boundary layers. Due to the strong pressure gradient across the polar front near the latitude y_2 in the TC layer above, the IW experiences a large eastward deflection at that latitude. The TC water is found above the IW everywhere south of y_2. But it is so thin over the ventilated area that most transport is taken place just outside this area, i.e., in the shadow area (Fig. 6). This fact might be related to the observed large southward extension of cold water mass off Korean coast and the consequent inhibition of the northward extension of TC (Hong *et al.*, 1984; Kim and Legeckis, 1986). For $w_0=2\times10^{-7}$ m/s and $y_e=0$, both ventilation of the IW and outcropping of the DW occur in much reduced area (Fig. 7). As in the previous case, the transport of the TC occurs mostly outside the ventilated area (Fig. 8). The model considered here is practically equivalent to the two-dimensional reduced gravity model in that the two-layer structure in the ventilated area is greatly dominated by the IW layer rendering it a single IW layer over the DW; likewise, in the shadow area, only the TC layer is in motion over the motionless DW. The reason why most TC (IW) transport occurs in the shadow (ventilated) zone can be explained as follows. Along the boundary between the shadow and ventilated zones, the IW has bottom depth H_0. Westward of this boundary, i.e., within the ventilated zone, this depth decreases because of the northward velocity of the IW. On the other hand, just west of this boundary, the IW should have thickness nearly the same as H_0 because of both the potential vorticity conservation and small change of f. It means that the layer thickness of TC almost vanishes over the ventilated zone, along with its gradient. In the ventilated zone, the velocity is nearly barotropic and the TC transport becomes negligible. For the wind forcing limited to the north of the polar front, i.e., for $y_e>y_2$, with w_0 kept the same, a wind-induced cyclonic circulation of the IW with outcropping of the DW appears only north of

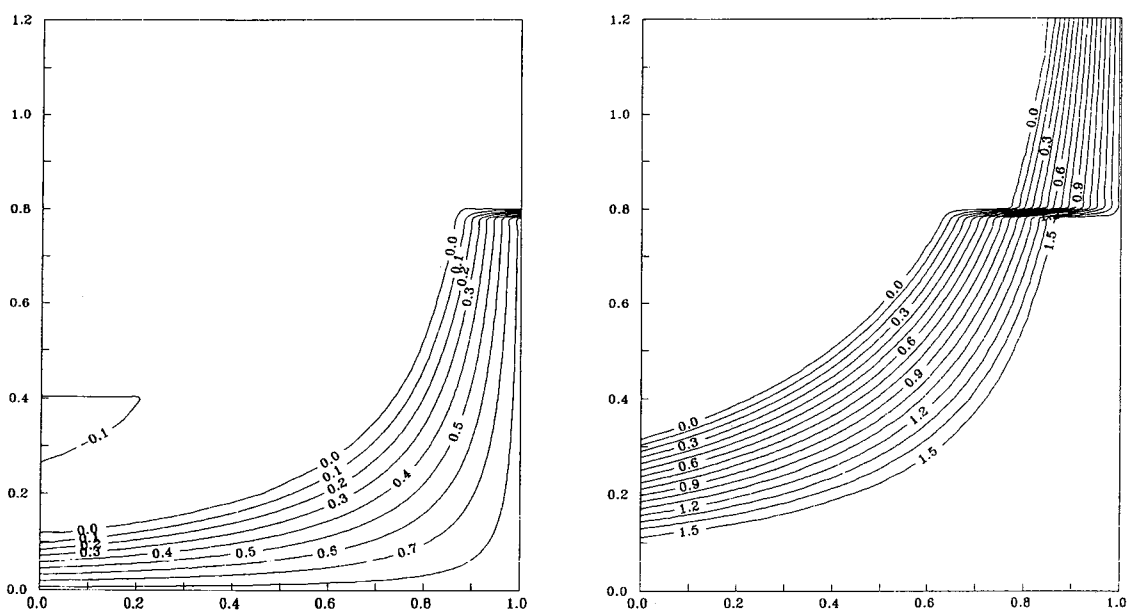

Fig. 6. Distributions of the transport streamfunction (in Sverdrup) of the TC(left) and IW (right) in the same coordinate system as in Fig. 5.

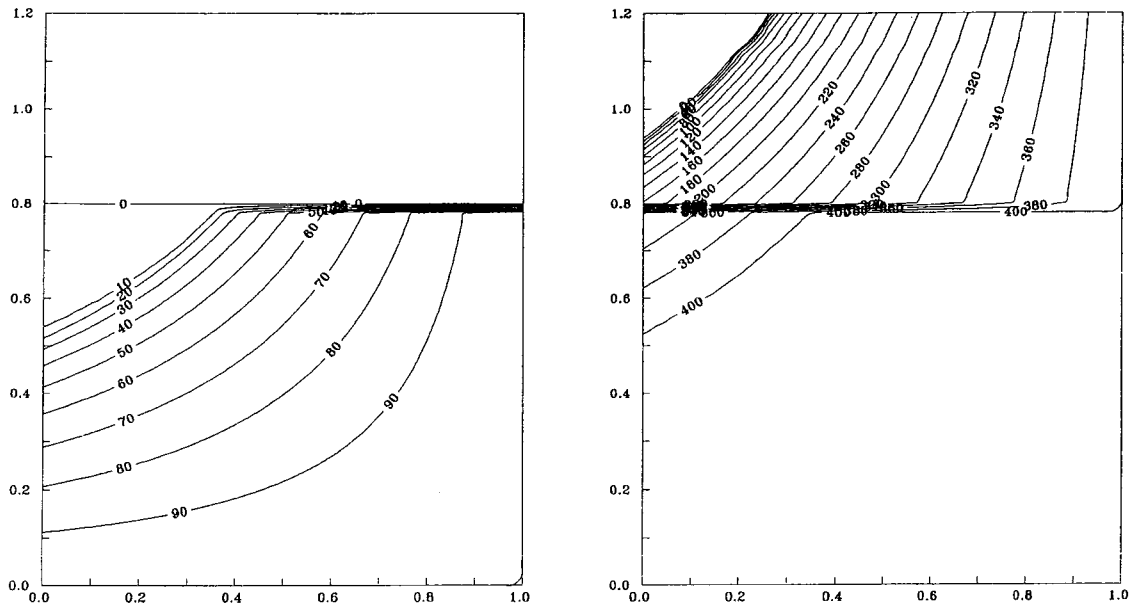

Fig. 7. Same as Fig. 5 except for $w_0=2\times10^{-7}$ m/s.

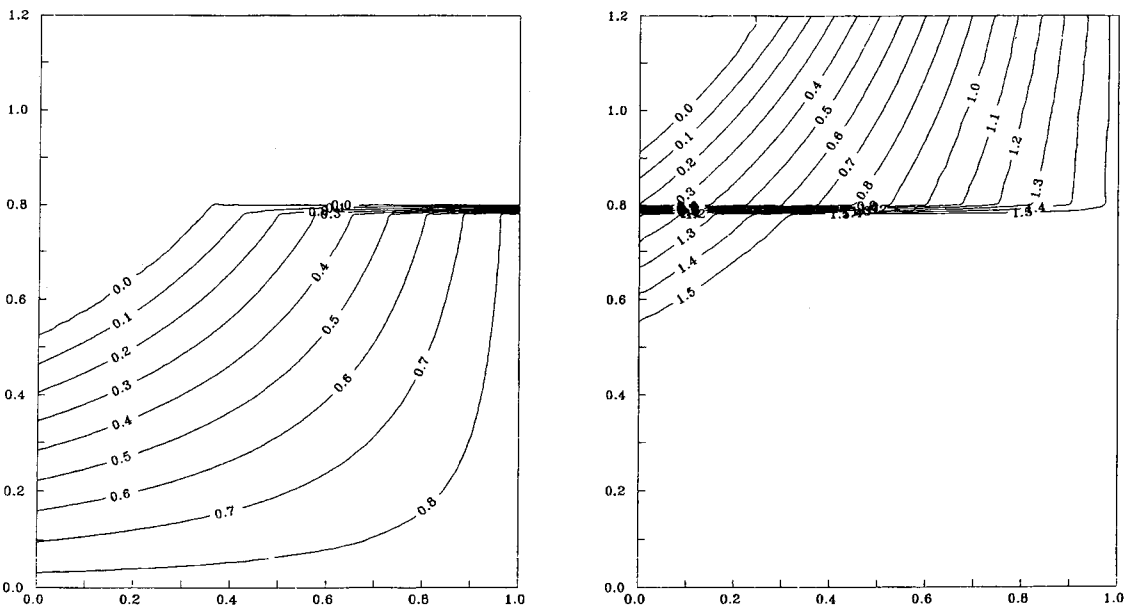

Fig. 8. Same as Fig. 6 except for $w_0=2\times10^{-7}$ m/s.

y_e (Fig. 9). South of y_e, it is the same as that without wind forcing which is already mentioned above. For $w_0=10^{-7}$ m/s and $y_e=0$, the Ekman pumping is not strong enough to create ventilation of the IW (Fig. 10). Outcropping of the DW does not occur either. The transport of the TC occurs mainly along the polar front as it does without the wind forcing (Fig. 10). The reduction of the ventilated zone with decreasing Ekman pumping may be explained as follows. In the region south of y_2, for weaker Ekman pumping, the TC transport becomes more zonal along the outcropping latitute. Because of the large interface depth change across the strong zonal current, it becomes hard for the IW crossing the current to conserve the potential vorticity (layer thickness).

It is quite difficult to say which one of above cases is most realistic because the wind condition is greatly variable in space and time. It seems that the ventilation is not so significant because the wind forcing is sufficiently strong only for a few months during one year. However, the model proposes a

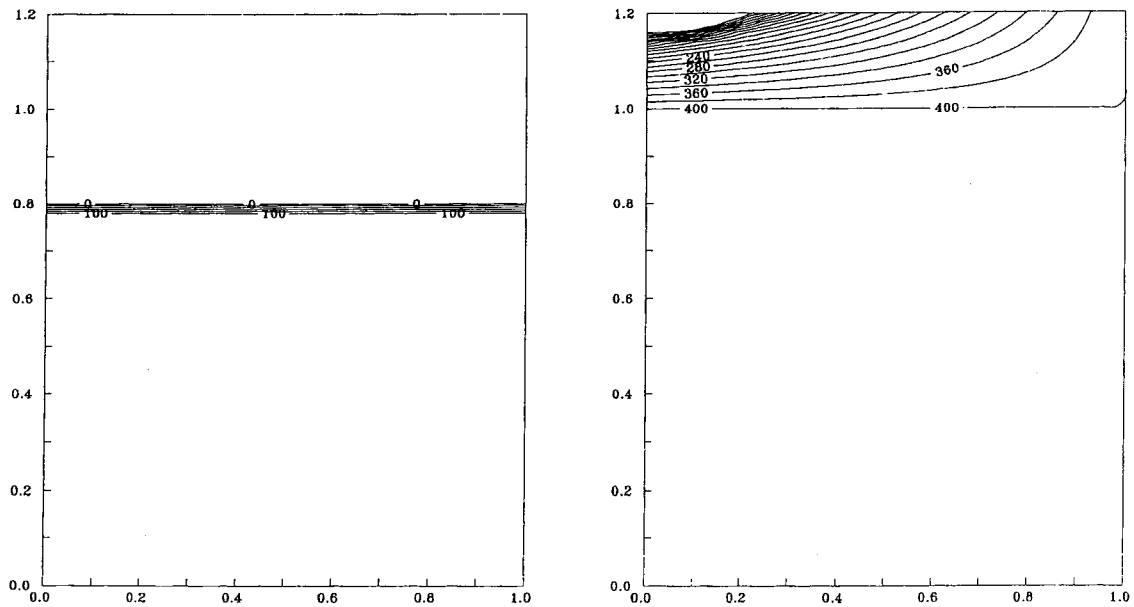

Fig. 9. Same as Fig. 7 except for y_e=1.0

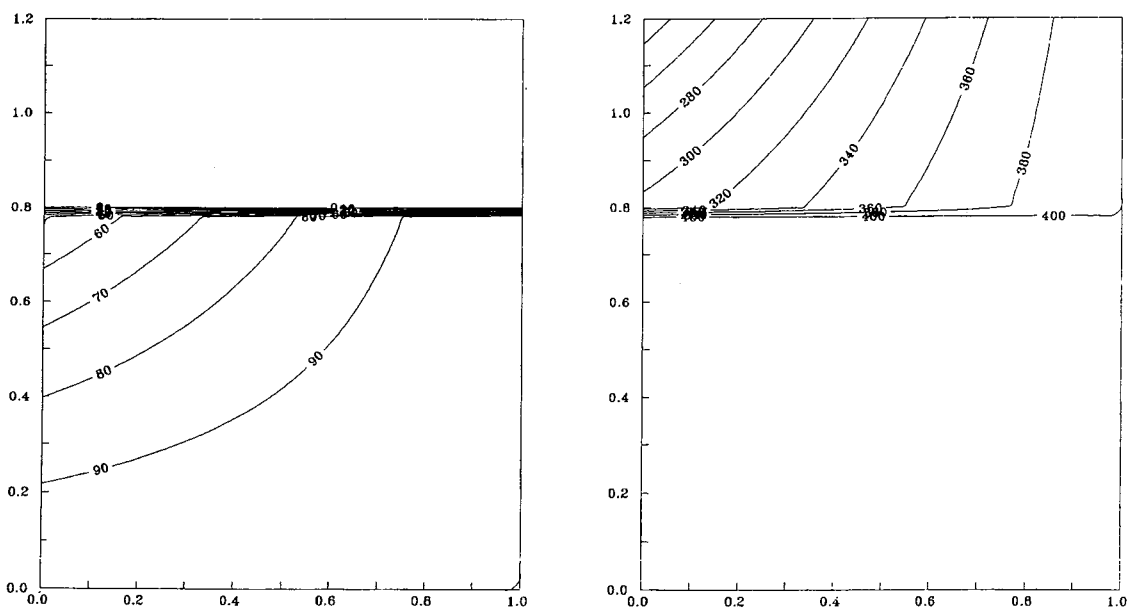

Fig. 10. Same as Fig. 5 except for w_0=10^{-7} m/s.

possible ventilation process of the intermediate circulation. It suggests that the first candidate area of the deep convection is the northwestern part of the basin as previous studies (Senjyu and Sudo, 1994; Seung and Yoon, 1995a) do. It also gives the same cyclonic circulation as in the numerical experiments (Seung and Kim, 1993; Seung and Yoon, 1995b) in the north of the basin. In the context of the model result, the submerging IW is richest in oxygen near the western boundary just south of the polar front. In fact, the IW found in the west is younger and therefore richer in oxygen than that found eastward (Kim and Chung, 1984). In contrary to the subduction, which is common in the ventilation of the subtropical gyre in the open ocean, it predicts an obduction across the polar front in the East Sea.

CONCLUDING REMARKS

The simple ventilation theory developed by LPS (1983) is applied to the East Sea by considering the

inflow-outflow condition which consists an important component in the surface circulation of the basin. The theory indicates many possibilities. The most probable candidate area of deep water formation is the northwestern part of the basin. The subsurface region where one can find the oxygen-rich IW might be the western part just south of the polar front as supported by observations (Kim and Chung, 1984). The IW, which is forced directly by the wind in the north, circulates cyclonically. It intrudes beneath the TC layer through the western boundary layer and finally outcrops to the north across the polar front by conserving the potential vorticity. The cyclonic circulation of the IW is also supported by hydrographic analyses (Senju and Sudo, 1994).

The results obtained in this study largely depend on the wind forcing. The magnitude of Ekman pumping, however, is variable in space and time so that any typical distribution pattern of Ekman pumping velocity can hardly be defined especially for the steady state problems like the one considered here. Besides, the model is incomplete in many aspects. It neglects the effects of convective mixed layer with variable depths. It assumes infinitely deep DW whereas the DW with finite depth would actually be ventilated when it is exposed to the wind forcing. The conservation of potential vorticity within the northern and western boundary layers has also to be checked. The model suggests southward submersion of the IW along the western boundary whereas observations by Cho and Kim (1994) indicate one more path of the IW from the northeast. Overall, this study predicts only the gross feature of what may happen in the intermediate layer. Although the results of this study cannot be taken for granted until they are supported by observational evidences, they may be served as a rough guide to more elaborate studies. A numerical model study focusing on this subject is now in progress.

ACKNOWLEDGEMENT

This study is supported by non directed research, fund, Korea Research Foundation (1995~1997) and, in part, by Basic Science Research Institute Program, Ministry of Education (1996).

REFERENCES

Cho, Y.-K. and K. Kim, 1994. Two modes of the salinity-minimum layer water in the Ulleung Basin. *La mer*, **32**: 271-278.

Hong, C.H., K.D. Cho and S.K., Yang, 1984. On the abnormal cooling phenomenon in the coastal areas of East Sea of Korea in summer 1981. *J. Oceanol. Soc. Korea*, **19**: 11-17.

Kang, Y.Q., 1988. On the formation of the East Korean Warm Current. *Ocean Res.*, **10**: 1-6.

Kim, K. and J.Y. Chung, 1984. On the salinity-minimum and dissolved oxygen-maximum layer in the East Sea(Sea of Japan). In: Ocean Hydrodynamics of the Japan and East China Seas, edited by T. Ichiye, Elsevier, Amsterdam.

Kim, K. and R. Legeckis, 1986. Branching of the Tsushima Current in 1981-83. *Progr. Oceanogr.*, **17**: 265-276.

Kim, C.H., H.J. Lie and K.S. Chu, 1991. On the Intermediate water in the southwestern East Sea(Sea of Japan). In: Oceanography of Asian Marginal Seas, edited by K. Takano, Elsevier, Amsterdam.

Luyten, J.R., J. Pedlosky and H. Stommel, 1983. The ventilated thermocline. *J. Phys. Oceanogr.*, **13**: 292-309.

Maizuru Marine Observatory, 1976. Oceanographic prompt reports, supplement for No. 290. Maizuru, Japan.

Moriyasu, S., 1972. The Tsushima Current. In: Kuroshio, edited by H. Stommel and K. Yoshida, Univ. of Tokyo Press.

Na, J.Y., J.W. Seo and S.K. Han, 1992. Monthly-mean sea surface winds over the adjacent seas of the Korea Peninsular. *J. Oceanol. Soc. Korea*, **27**(1): 1-10.

Senjyu, T. and H. Sudo, 1994. The Upper Portion of the Japan Sea Proper Water; Its source and circulation as deduced from isopycnal analysis. *J. Oceanogr.*, **50**: 663-690.

Seung, Y.H., 1992. A simple model for separation of East Korean Warm Current and formation of North Korean Cold Current. *J. Oceanol. Soc. Korea*, **27**(3): 189-196.

Seung, Y.H. and K. Kim, 1993. A numerical modeling of the East Sea circulation. *J. Oceanol. Soc. Korea*, **28**(4): 292-304.

Seung, Y.H. and J.H. Yoon, 1995a. Some features of winter convection in the Japan Sea. *J. Oceanogr.*, **51**: 61-73.

Seung, Y.H. and J.H. Yoon, 1995b. Robust diagnostic modeling of the Japan Sea circulation. *J. Oceanogr.*, **51**: 421-440.

Uda, M., 1934. Oceanographic conditions of the Japan Sea and its adjacent waters. *J. Imp. Fisher. Exp. St.*, **7**: 91-191. (in Japanese).

Yoon, J.H., 1982a. Numerical experiment on the circulation in the Japan Sea, Part I: Formation of the East Korean Warm Current. *J. Oceanogr. Soc. Japan*, **38**: 43-51.

Yoon, J.H., 1982b. Numerical experiment on the circulation in the Japan Sea, Part III: Mechanism of the Nearshore Branch of the Tsushima Current. *J. Oceanogr. Soc. Japan*, **38**: 125-130.